AUT Journal of Electrical Engineering

AUT J. Elec. Eng., 51(2) (2019) 171-186
DOI: 10.22060/eej.2019.16219.5278

A Thorough Comparative Analysis of PI and Sliding Mode Controllers in Permanent Magnet Synchronous Motor Drive Based on Optimization Algorithms

F. Khorsand, R. Shahnazi* , E. Fallah

Department of Electrical Engineering, Faculty of Engineering, University of Guilan, Rasht, Iran

ABSTRACT: In this paper, the speed tracking for permanent magnet synchronous motor (PMSM) in field oriented control (FOC) method is investigated using linear proportional-integral (PI) controller, sliding mode controller (SMC) and its advanced counterparts. The advanced SMCs considered in this paper are fuzzy SMC (FSMC) and sliding mode controller with time-varying switching gain (SMC+TG) which can effectively cope with chattering, an inherent harmful phenomenon in SMC. Regardless of all the works done to replace PI controller with SMC and its advanced counterparts, a thorough comparison of the PMSM drive behavior under mentioned controllers is still missing. This paper attempts to fill in this gap, by providing a fair and in-depth comparison of the PMSM drive operation by using PI and sliding mode speed controllers. In this paper, in order to design and provide a fair framework for comparison the performance and robustness of these four controllers a suitable cost function is defined to manage the performance effectively. Thus, based on this cost function a nonlinear optimization problem is defined. To solve the optimization problem and consequently derive the optimal values for the parameters of the controllers, particle swarm optimization (PSO) and grey wolf optimization (GWO) algorithms are employed. The performance and robustness of the PMSM drive using four optimal controllers are studied in the presence of different conditions and uncertainties. Numerical results demonstrate that SMC and its advanced counterparts cannot offer the superior behavior for all conditions and their superiority is less than it is often stated in the literature.

Review History:
Received: 2019-04-26
Revised: 2019-09-12
Accepted: 2019-09-13
Available Online: 2019-12-01

Keywords:
Sliding Mode Controller
Fuzzy Logic
PI Controller
Particle Swarm Optimization
Grey Wolf Optimization
Permanent Magnet Synchronous Motor Drive

1. Introduction

Adjustable speed drives (ASD) are equipment used to control motor speed which play an important role in electromechanical energy conversion and are seen in many of our daily appliances, such as cooling fans, washing machines, computers and many other devices [1]. In the past, direct current (DC) motors were commonly used in such drives, but these motors have some disadvantages such as high cost, high rotor inertia and maintenance problems associated with commutators and brushes. Using Alternative current (AC) motors in ASDs, improves the mentioned problems for DC motors [2]. In the last few decades, with advances in electronic components, semiconductor switches and improvements in various control techniques, AC drives have been preferred over DC drives [1, 3]. Permanent magnet synchronous motor (PMSM) is one of the AC motors that is widely used in the industry due to its unique features such as high performance, low inertia, low noise, high output torque, simple structure and high power density [4]. In ASDs, it is vital to employ a control method that responds quickly and accurately to speed changes and saves the energy. To fulfill these objectives field oriented control (FOC), which provides independent control of flux and torque is a popular and commonly used control method in controlling AC drives [3]. FOC was firstly used to control the induction motor drives and due to its success, it was also applied to synchronous motor drives like PMSM drives [5]. In the FOC method, linear proportional-integral (PI) controller is considered as a standard controller in the control loops. Determining the control parameters and inability to deal with uncertainties in the system makes it difficult to work with PI controllers. Along with the progress in control areas, the replacement of PI controller with nonlinear controllers in the FOC has been considered [6]. Until now, various nonlinear control methods such as adaptive control, predictive control and sliding mode controller (SMC) have been proposed to improve the control of PMSM drives. Among them, SMC is an effective and suitable control method because it is not sensitive to parametric changes, is robust to external disturbances and has fast dynamic response [7].

The use of SMC in a system, although provides high robustness for the system against uncertainties, it causes the occurrence of the harmful phenomenon called chattering [8-11]. Many efforts have been made to eliminate this defect and various techniques have been proposed, such as fixed boundary layer [11, 12], variable boundary layer [13, 14], modification of the reaching law [9], the combination of fuzzy logic theory with sliding mode control [15-17], and the use of

*Corresponding author's email: shahnazi@guilan.ac.ir

high order sliding mode control [18].

Along with the research to improve the performance of SMC, its application to control of AC drives such as the PMSM drives has been improved [19-26]. In these works, the PI controller in speed control loop is replaced by SMC and its advanced counterparts. In [19], SMC is considered with a fixed boundary layer. In [20], a new reaching law is considered which by preserving the benefits of conventional SMC, results in a continuous control law. Wang et al. in [21] presented a new exponential reaching law that is a function of state variables and causes exponential decaying boundary layer. In [22], a new reaching law is presented such that the switching gain of the discontinuous term varies with the system error and distance from the sliding surface. This controller is called sliding mode controller with time-varying switching gain (SMC+TG). In order to improve the dynamic response of PMSM drives in [23], a fuzzy SMC (FSMC) is proposed. To achieve a compromise between the chattering and the reaching time to the sliding surface, a fuzzy system, whose output is the switching gain has been designed. In [24], to control the speed of the PMSM, an integral SMC is considered such that to overcome the chattering, a fuzzy controller is embedded in an inner feedback loop to improve the control signal. To reduce the torque ripple and at the same time improve the robustness of the PMSM drive in [25], an adaptive SMC is proposed. The adaptive mechanism is used to estimate the lumped uncertainties and consequently mitigates the chattering. In [26], by combining the merits of deadbeat predictive current control and sliding mode the performance and robustness of the PMSM drive have been improved. In order to suppress the chattering higher order SMC method has been utilized.

One of the important approaches is comparative studies of different controllers for speed control of PMSM drive. These studies are vital since they give the specific advantages and disadvantages of the controllers. They also determine a measure for the strength of the controllers in performance and robustness. To this end, [6, 27] have studied the comparative analysis between fuzzy logic and PI controllers, while [28] compares PI, fuzzy logic and conventional sliding mode controllers. With the thorough comparisons in [6], it is shown that fuzzy logic controller is not a superior controller for all the cases, which is inconsistent with the most of the results in the literature due to inadequate comparisons. In other words, in some cases PI controller has more enhanced speed response. However, the studies in [27, 28] due to using inadequate cases are incomplete and do not give a thorough comparison between different controllers.

To our best knowledge, the thorough comparison of the PMSM drive behavior under PI controller, SMC and its advanced counterparts have not been considered, yet. Here, we consider PI controller, SMC, FSMC and SMC+TG in speed control loop. Selecting the parameters values of a controller highly affects its behavior. Therefore, in order to present a common method to select the parameters values of the controllers and at the same time to provide a fair framework to compare these four controllers under different situations, in this paper, an optimization method is proposed. Since the objective of speed control loop is to reach the desired speed effectively, here we consider integral absolute speed tracking error as the cost function. The optimization problem is to determine the unknown parameters of the each controller by minimizing this cost function. However, the present optimization problem is highly nonlinear and therefore a closed-form solution cannot be obtained. Thus, the meta-heuristic methods are considered to solve this highly nonlinear optimization problem. In this paper, particle swarm optimization (PSO) and gray wolf optimization (GWO) algorithms as two successful algorithms in recent applications are considered. The proposed framework not only derives the unknown parameters of the controllers but also guarantees the optimality of the controllers based on the stated cost function. Meanwhile, it provides a fair background to compare these four controllers in terms of performance and robustness. Afterwards, the performance of the proposed optimal controllers is compared using different criteria. Besides, the robustness of them is studied under different uncertainties such as changing in reference speed, parametric changes and the presence of unknown load torque. Simulation results demonstrate that a single controller cannot offer the best performance for all conditions. However, optimal SMC, optimal FSMC and optimal SMC+TG can achieve the superior robustness in the presence of uncertainties in comparison to optimal PI controller. Nonetheless, again none of these four optimal controllers wins the best robustness in all conditions and based on the kind of uncertainty one controller leads the way.

The paper is organized as follows: In Section 2, the PMSM model is introduced in the d-q reference frame, SMC, SMC+TG and FSMC are introduced. Meanwhile, the PSO and GWO algorithms are briefly described. The proposed optimization framework is stated in Section 3. In Section 4, the simulation results are studied and a thorough comparison of the proposed optimal controllers in terms of performance and robustness are accomplished. Finally, Section 5 concludes the paper with the key points of the proposed comparative method discussed.

2. Preliminaries and controllers

2.1. Model of PMSM

The mathematical model for surface PMSM in the rotating d-q reference frame is as follows ([22, 29]):

$$\begin{cases} \dfrac{di_d}{dt} = \dfrac{1}{L}(v_d - R_s i_d + \omega_e L i_q) \\ \dfrac{di_q}{dt} = \dfrac{1}{L}(v_q - R_s i_q - \omega_e L i_d - \omega_e \phi_{mg}) \\ \dfrac{d\omega_e}{dt} = \dfrac{p}{J_m}(T_e - \dfrac{B_v}{p}\omega_e - T_L) \end{cases} \quad (1)$$

$$T_e = \frac{3}{2} p \phi_{mg} i_q$$

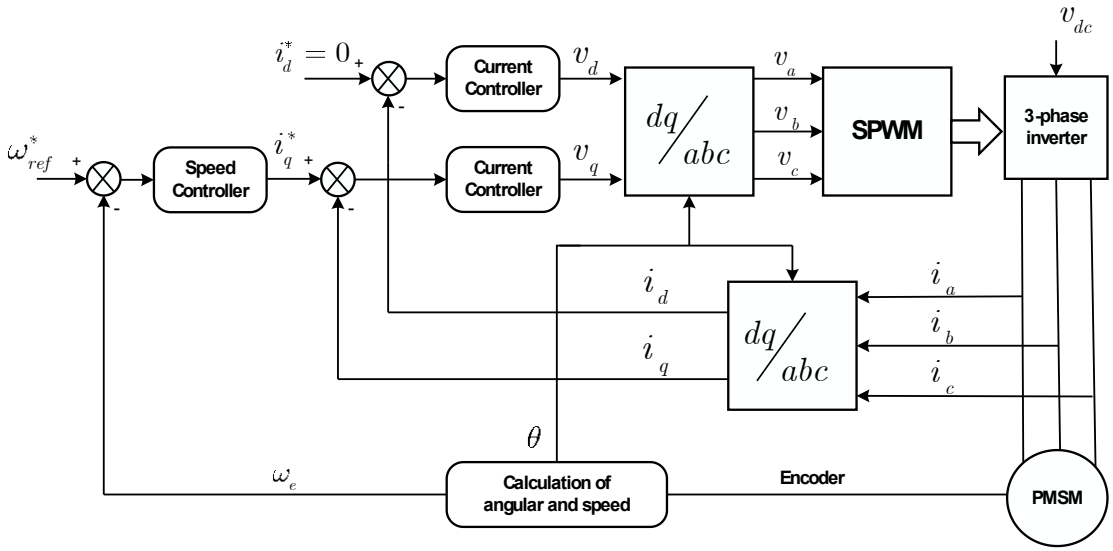

Fig. 1. Control scheme for the speed control of PMSM

where v_d, v_q, i_d and i_q are voltages and currents of stator in d and q directions respectively. R_s, L, ω_e and ϕ_{mg} are respectively the stator resistance, stator inductance, electrical angular speed and flux linkage of permanent magnet. Electromagnetic torque, external load torque, number of pole pairs, the moment of inertia and viscous friction coefficient are represented by T_e, T_L, p, J_m and B_v, respectively. In this paper, the block diagram in Fig. 1 is considered to control the speed of PMSM called FOC [1-3].

As can be seen from Fig. 1, there are two control loops for d-axis and q-axis currents and a control loop for the motor speed. Reference d-axis current set to zero for maximizing torque. In this paper, sine pulse width modulation (SPWM) is considered to generate the gate signals for inverter. The current loops are related to the electrical part of the motor and the speed loop is associated to the mechanical part.

2.2. Sliding mode controller (SMC)

Sliding mode controller drives the states of a system to a specific surface called sliding surface, and when the states reach the sliding surface, keeps them near this surface. Thus, design of the SMC consists of two steps; the first step is the design of sliding surface, and the second step is to derive a control law that leads the states of the system to the sliding surface [30]. Consider the following theorem [22, 31].

Theorem 1. Consider the PMSM model in , if i_q^* in Fig.1 is selected as follows

$$i_q^* = \frac{2J_m}{3p^2\phi_{mg}}\left(\frac{B_v}{J_m}\omega_e + \dot{\omega}_{ref}\right) + k_c \operatorname{sgn}(s), \tag{2}$$

where k_c is a positive constant, then the motor electrical angular speed (ω_e) tends the desired speed (ω_{ref}) asymptotically by considering $s = e = \omega_{ref} - \omega_e$ as the sliding surface.

Remark 1. The discontinuous term $k_c \operatorname{sgn}(s)$ is able to lead the state trajectories to the sliding surface and guarantees robustness of SMC. However, it causes the harmful phenomenon called chattering [21].

2.3. Sliding mode controller with time-varying switching gain (SMC+TG)

To mitigate the chattering, while maintaining desirable tracking a new reaching law is proposed by modification of . Now, the following theorem is concluded from the results in [22].

Theorem 2. Consider the PMSM model in , if i_q^* in Fig.1 is selected as follows

$$i_q^* = \frac{2J_m}{3p^2\phi_{mg}}\left(\frac{B_v}{J_m}\omega_e + \dot{\omega}_{ref}\right) + \frac{k_t}{\left[\varepsilon + \left(1 + 1/\left|e\right| - \varepsilon\right)\exp\left(-\delta\left|s\right|\right)\right]}\operatorname{sgn}(s), \tag{3}$$

where $k_t > 0$, $\delta > 0$, $0 < \varepsilon < 1$, then the motor electrical angular speed (ω_e) reaches to an arbitrarily neighborhood of the desired speed (ω_{ref}) by considering $s = e = \omega_{ref} - \omega_e$ as the sliding surface.

Remark 2. In Theorem 2, if $|s|$ increases, i.e., when the states are far from the sliding surface, the switching gain converges to $\frac{k_t}{\varepsilon}$, which is greater than k_t and thus the reaching time is decreased. As $|s|$ decreases, then the switching gain will converge to $\frac{k_t|e|}{1+|e|}$, so with approaching the sliding surface and decreasing $|e|$, the value of the switching gain also converges to zero, and chattering is alleviated, effectively.

2.4. Fuzzy sliding mode controller (FSMC)

Fuzzy set theory was presented in 1965 by Lotfi Zadeh and

has been used in many areas such as control, communication, production of integrated circuits, medical and psychological fields [32]. One of the most important applications of fuzzy logic has been in the field of control [15]. Fuzzy systems are knowledge-based or rule-based systems, so at the beginning the suitable If-Then rules should be derived. In order to alleviate the chattering, fuzzy logic can be used to derive the k_c effectively. It is known that if the system trajectory is far from the sliding surface, selecting a large value for k_c, moves system trajectory to the sliding surface quickly. On the other hand, to mitigate the chattering, when the system trajectory approaches the sliding surface, the value of the k_c should gradually decreases. This information can be converted into If-Then rules.

In this paper, a mamdani fuzzy system is designed to determine k_c [33]. The singleton fuzzifier, center average defuzzifier and product inference engine are considered. The input to the fuzzifier is the sliding surface and the output of the defuzzifier is k_c. The fuzzy rules in the fuzzy rule base are considered as follow [33]:

If s is NB Then k_c is VH
If s is NM Then k_c is H
If s is NS Then k_c is L
If s is ZO Then k_c is VL
If s is PS Then k_c is L
If s is PM Then k_c is H
If s is PB Then k_c is VH

where, NB, NM, NS, ZO, PS, PM and PB, respectively, denote negative big, negative medium, negative small, zero, positive small, positive medium, and positive big for input membership functions of the fuzzy system. Meanwhile, VL, L, H, and VH, respectively, account for very low, low, high, and very high for output membership functions of the fuzzy system.

2.5. Particle swarm optimization (PSO) algorithm

Particle swarm optimization (PSO) algorithm, was introduced by Russell Eberhart and James Kennedy [34]. They introduced this algorithm with inspiring from some of the collective animal behavior. For example for finding food, the member who has the best position to the source will inform the other members of the group. This exchange of information continues until the source of food is found [35]. In the PSO algorithm, particle swarm includes n particles and the position and speed of each particle are updated as follows [36]:

$$V_i^{k+1} = \omega V_i^k + c_1 r_1 \left(P_i^k - x_i^k\right) + c_2 r_2 \left(P_g^k - x_i^k\right) \quad (4)$$

$$x_i^{k+1} = x_i^k + V_i^{k+1} \quad (5)$$

where x_i^k and v_i^k are the position and speed of i-*th* particle at k-th iteration, respectively. P_i^k is the best answer of i-*th* particle, and P_g^k expresses the best common response of all particles. In addition, ω stands for inertia factor; r_1 and represent random numbers in [0,1]; c_1 and c_2 determine learning rates in the direction of personal best (P_i^k) and global best (P_g^k), respectively.

2.6. Grey wolf optimization (GWO) algorithm

Gray wolf optimization (GWO) algorithm was introduced in 2014 [37]. This algorithm is inspired by the group life of gray wolves. Wolves belonging to a group are sorted in order of importance: alpha, beta, delta and omega. To model the hunting process, it is assumed that the answer to the problem is the position of the prey, and the best option for solving the problem are, the alpha, beta and delta particles, which represent the alpha, beta and delta wolves respectively. Omega particles, as the representative of omega wolves, are the last option to solve the problem. For modeling hunting operations in mathematical form, the following equations are introduced:

$$\begin{aligned} &\vec{D} = \left|\vec{C}.\vec{X}_P(t) - \vec{X}(t)\right| \\ &\vec{X}(t+1) = \vec{X}_P(t) - \vec{A}.\vec{D} \end{aligned} \quad (6)$$

where, t indicates the current iteration, $|\cdot|$ is absolute value, $\vec{X}_P(t)$ and $\vec{X}(t)$ indicate position vector of the prey and a gray wolf, respectively at t-th iteration, respectively. Meanwhile, $\vec{A}$ and $\vec{C}$ are coefficient vectors calculated as follows:

$$\vec{A} = 2\vec{a}.\vec{r}_1 - \vec{a} \quad (7)$$

$$\vec{C} = 2.\vec{r}_2 \quad (8)$$

where r_1 and r_2 represent random numbers in [0,1] and $\vec{a}$ linearly decreases from 2 to zero during the iterations. From (6), the position of the prey should be known, however, accurate information on the prey position is not available. Therefore, the following equations are used to indicate the mathematical model of hunting in general terms.

$$\begin{aligned} &\vec{D}_\alpha = \left|\vec{C}_1.\vec{X}_\alpha - \vec{X}\right|, \vec{D}_\beta = \\ &\left|\vec{C}_2.\vec{X}_\beta - \vec{X}\right|, \vec{D}_\delta = \left|\vec{C}_3.\vec{X}_\delta - \vec{X}\right| \end{aligned} \quad (9)$$

$$\begin{aligned} &\vec{X}_1 = \vec{X}_\alpha - \vec{A}_1.(\vec{D}_\alpha), \vec{X}_2 = \\ &\vec{X}_\beta - \vec{A}_2.(\vec{D}_\beta), \vec{X}_3 = \vec{X}_\delta - \vec{A}_3.(\vec{D}_\delta) \end{aligned} \quad \backslash^* \quad (10)$$

$$\vec{X}(t+1) = \frac{\vec{X}_1 + \vec{X}_2 + \vec{X}_3}{3} \quad \backslash^* \quad (11)$$

where, $\vec{X}_{\alpha}$, $\vec{X}_{\beta}$, $\vec{X}_{\delta}$ and $\vec{X}$ indicate the position vector of the alpha, beta, delta wolves and estimate of prey, respectively.

3. Proposed comparative method

Consider the block diagram in Fig. 1 to control the speed of PMSM. Generally, the time constant of the electrical part is much smaller than the mechanical part. Thus, for the fast current loops the conventional PI controller is considered. However, PI controller, SMC, SMC+TG and FSMC are proposed for the mechanical part, i.e., the speed controller in Fig. 1. Therefore, four different scenarios are considered:

Scenario I. The controllers for speed and currents are PI. Each PI controller has two parameters and thus, we have six parameters to be tuned.

Scenario II. The controller for speed is SMC and the PI controller is used for the currents. Based on discussions in Subsection 2.2, SMC has just one parameter and each PI controller contains two parameters, thus we have five parameters to be tuned.

Scenario III. The controller for speed is considered to be FSMC and the PI controller is used for currents. For fuzzy rules as discussed in Subsection 2.4 it is assumed that the center of each output membership function is unknown and thus, FSMC has four parameters to be tuned. Meanwhile, each PI controller in current loops has two parameters. Thus, totally in the third scenario we have eight parameters to be tuned.

Scenario IV. The speed controller is SMC+TG and again the PI controller is used for currents. Based on discussions in Subsection 2.3, SMC+TG has three parameters which by adding four parameters of the PI controllers we totally have seven parameters to be tuned.

Parameters of the controllers have deep influence in their ability for performance and robustness. One may choose parameters by trial and error, however; this is not only a difficult task but also does not provide a fair framework to compare the performance and robustness of the controllers. In this paper, in order to have a fair framework for comparing the performance and robustness of the PI controller, SMC, SMC+TG and FSMC and at the same time derive the *sub-optimal* parameters of the controllers, for each controller the following optimization problem is considered:

$$\min_{\substack{\text{Controller}\\ \text{Parameters}}} IAE = \min_{\substack{\text{Controller}\\ \text{Parameters}}} \int_0^{\infty} \left|e(t)\right| dt \qquad (12)$$

where $e(t)$ is the speed tracking error and IAE stands for integral absolute speed tracking error. Thus, minimizing IAE leads to minimizing the speed tracking error, which is the ultimate goal for controller design. Considering (12) , this is a highly nonlinear optimization problem, which cannot be easily solved and does not have a closed-form solution. It has been shown in recent years that meta-heuristic optimization methods are useful and effective in solving nonlinear optimization problems [38]. From (6), the position, PSO and GWO algorithms discussed in Subsections 2.5 and 2.6, respectively as two effective methods are utilized.

Table 1. Parameters of PMSM [22]

Stator phase resistance	$R_s = 3.5\,\Omega$
Stator inductance	$L = 11.5\times10^{-3} H$
Viscous friction coefficient	$B_v = 0.00001\,N.m.s\,/\,rad$
Moment of inertia	$J_m = 0.00044\ Kg.m^2$
Flux linkage of permanent magnet	$\phi_{mg} = 0.107\ wb$
Number of pole pairs	$p = 3$

Table 2. PSO Parameters [39]

Learning rate in local direction	$c_1 = 1.4961$
Learning rate in global direction	$c_2 = 1.4961$
Inertia coefficient	$\omega = 0.7298$

The remaining of the paper is summarized as follows: In Section 4, thorough comparative studies of the proposed scenarios under proposed fair framework are accomplished. In Subsection 4.1, the optimization problem (12) is solved for each scenario using PSO and GWO algorithms for the desired speed 1000rpm. For the proceeding analyses, the best solution derived from these two algorithms will be considered as the controllers' parameters. In Subsection 4.2, based on chosen solutions the performance of the proposed scenarios is studied using different criteria. Subsection 4.3, studies the robustness of the proposed scenarios under different uncertainties.

4. Thorough comparative analysis of the proposed scenarios

4.1. Choosing the optimization algorithm

Here, to solve the optimization problem in (12), PSO and GWO algorithms are considered. The best solution derived from these two algorithms will be used as the controllers' parameters for the proceeding analyses. For simulation and without loss of generality the desired initial speed of the motor is considered at 1000rpm. For both algorithms, the number of iterations and the number of particles/number of grey wolves are considered 40 and 20, respectively. The parameters of the PMSM for the simulations and parameters of the PSO algorithm are listed in Tables 1 and 2, respectively.

By applying the proposed comparative method described in Section 3, the sub-optimal control parameters for scenarios I-IV are respectively shown in Tables 3-6. In these tables, kp_s, kp_d and kp_q are the proportional parameters of the PI controllers in speed, d-axis current and q-axis current control loops, respectively. Meanwhile, the integral parameters of the PI controllers in speed, q-axis current and d-axis current control loops are respectively ki_s, ki_q, ki_d. In order to put the proposed method into a challenging experiment, the range of

Table 3. Sub-optimal values of the parameters for the controllers in scenario I

PSO algorithm		GWO algorithm	
kp_s	0.5074	kp_s	0.4481
ki_s	1.6031	ki_s	2.2783
kp_d	20	kp_d	16.1830
ki_d	11.5345	ki_d	3.6362
kp_q	15.4789	kp_q	5.0143
ki_q	4.4902	ki_q	7.6466

Table 4. Sub-optimal values of the parameters for the controllers in scenario II

PSO algorithm		GWO algorithm	
k_c	20	k_c	20
kp_d	19.7117	kp_d	20
ki_d	11.7281	ki_d	12.8332
kp_q	9.3064	kp_q	20
ki_q	6.2438	ki_q	4.4167

Table 5. Sub-optimal values of the parameters for the controllers in scenario III

PSO algorithm		GWO algorithm	
$center_{VL}$	3.1411	$center_{VL}$	3.2198
$center_{L}$	8.7526	$center_{L}$	6.0231
$center_{H}$	11.1258	$center_{H}$	10.9802
$center_{VH}$	20	$center_{VH}$	20
kp_d	20	kp_d	20
ki_d	7.1389	ki_d	12.3309
kp_q	15.4757	kp_q	5.2554
ki_q	7.1308	ki_q	4.2388

Table 6. Sub-optimal values of the parameters for the controllers in scenario IV

PSO algorithm		GWO algorithm	
k_t	11.8189	k_t	14.8969
δ	9.2282	δ	13.8796
ε	0.3913	ε	0.5
kp_d	19.5776	kp_d	20
ki_d	8.4731	ki_d	3.9201
kp_q	10.8641	kp_q	1.54
ki_q	11.4530	ki_q	11.8616

variations of the PI parameters for currents control is selected in [0,20] for all scenarios. For other control parameters in scenarios I-IV, the ranges of variations are considered as follows:

Scenario I. The range of variations of PI parameters in speed control loop, are selected in [0,20].

Scenario II. The range of variations for k_c the parameter of SMC is considered in [0,20].

Scenario III. The range of variations for k_c in scenario II ([0,20]), is divided to four parts such that each part belongs to an output membership function of the fuzzy system. So the range of variations for $center_{VL}$, $center_{L}$, $center_{H}$, and $center_{VH}$ which are centers of output membership functions (VL, L, H and VH), are respectively chosen in [0,5], [5,10], [10,15] and [15,20]. Indeed, the value of k_c in scenario III is not constant and FSMC is allowed to select any values in [0,20] for k_c. The input membership functions of the fuzzy system are depicted in Fig. 2.

Scenario IV. The range of variations for k_t is considered in [0,20], just like k_c. Accordance to Subsection 2.3, since $\delta > 0$ and $0 < \varepsilon < 1$, the range of variations for δ and ε are selected in [0,20] and [0,1], respectively.

The Convergence curves of PSO and GWO algorithms in solving optimization problem (12) using the four controllers i.e., PI controller, SMC, FSMC and SMC+TG in speed control loop (scenarios I-IV) are respectively demonstrated in Figs. 3-6.

To select the results derived by PSO or GWO algorithms, the values of IAE cost function for PSO and GWO algorithms are listed in Table 7. Considering Figs. 3-6 and Table 7, it can be concluded that using each of the four controllers in the speed control loop, the values of IAE cost function obtained by PSO and GWO algorithms are very close. This verifies that optimization has been correctly converged. Therefore, in order to check the performance and robustness of the four speed controllers (i.e., four scenarios), the two classes of parameters derived from PSO and GWO algorithms, respectively can be used. However, the values recorded for the IAE cost function in Table 7 indicate that the GWO algorithm has been more successful in reducing the value of the cost function. In addition, Figs. 3-6 reflect that GWO algorithm has converged faster than PSO algorithm. Therefore, the parameters extracted by GWO algorithm are used for proceeding studies.

4.2. Performance Analysis

Based on the discussions in Subsection 4.1, the sub-optimal parameters recorded in Tables 3-6 that are derived by the GWO algorithm, are used to evaluate the performance of the PMSM drive system. Figs. 7-9 respectively demonstrate speed, reference q-axis current and electromagnetic torque for all scenarios. The characteristics of the speed curve including: settling time (T_s), rise time (T_r), percentage of maximum overshoot (%Os) and absolute steady-state error (|ess|) are shown in Table 8. It should be noted that the values recorded for T_r and T_s for all the tables presented in this paper are in milliseconds (msec). Besides, *IAC* in Table 8, is a measure for control effort which is $\int_0^\infty |u(t)|dt$ and 2% criterion is used to

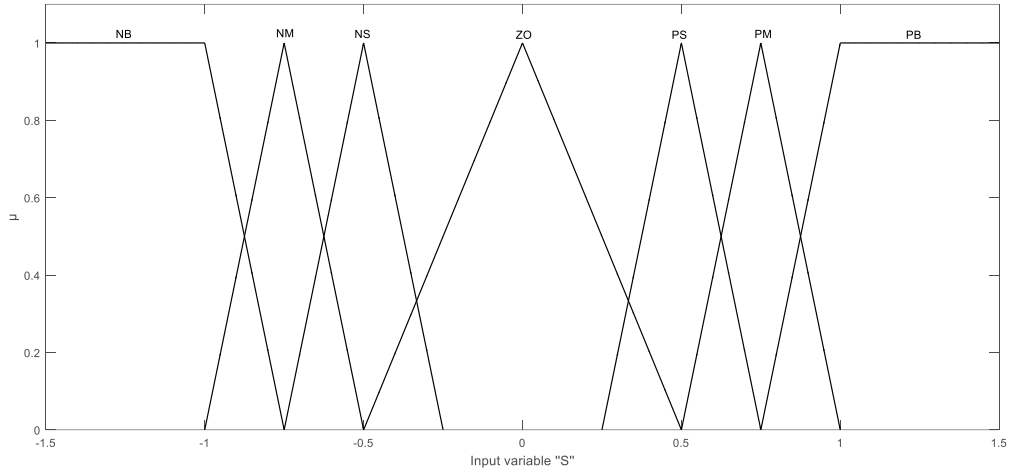

Fig. 2. Input membership functions of the fuzzy system.

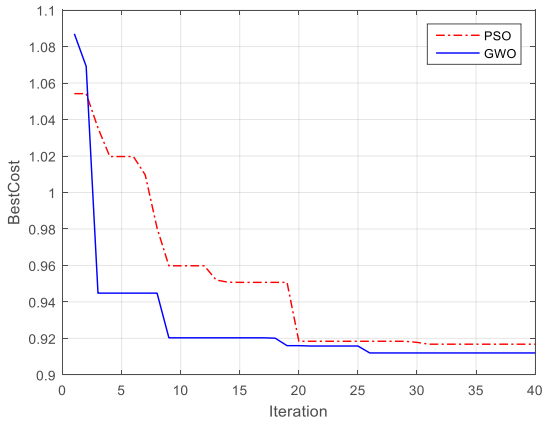

Fig. 3. Convergence curves of PSO and GWO algorithms by considering the PI controller in the speed control loop (Scenario I)

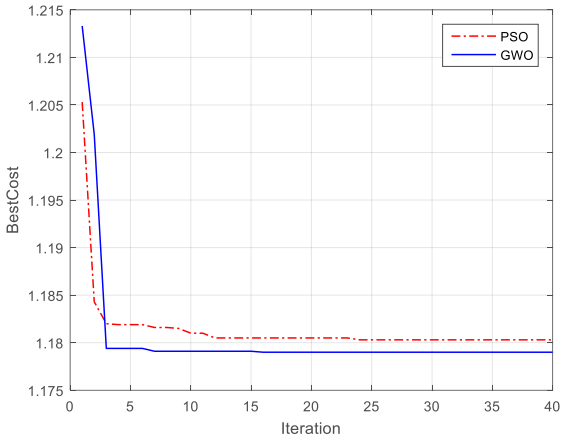

Fig. 5. Convergence curves of PSO and GWO algorithms by considering the FSMC in the speed control loop (Scenario III)

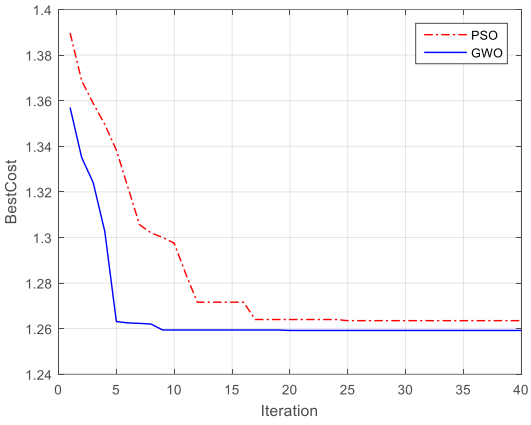

Fig. 4. Convergence curves of PSO and GWO algorithms by considering the SMC in the speed control loop (Scenario II)

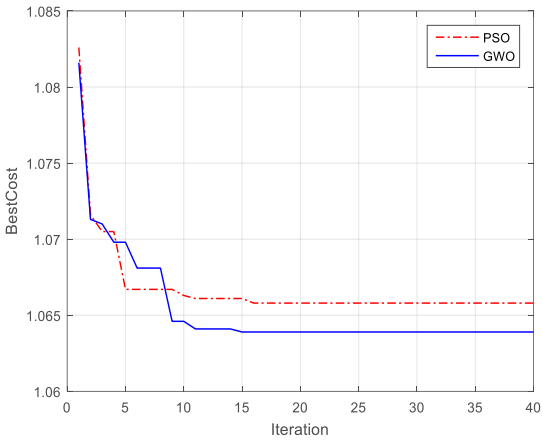

Fig. 6. Convergence curves of PSO and GWO algorithms by considering the SMC+TG in the speed control loop (Scenario IV)

calculate T_s.

The results of Table 8 show that when the PI controller in speed control loop is replaced by SMC, FSMC and SMC+TG (i.e., using scenarios II-IV instead of scenario I), it causes to increase in T_r, T_s, $\%O_s$ and IAC and it just decreases $|e_{ss}|$. Therefore, one cannot claim that PI controller has worse

Table 7. The values of IAE cost function for all the four scenarios based on PSO and GWO algorithms

	PI controller (Scenario I)	SMC (Scenario II)	FSMC (Scenario III)	SMC+TG (Scenario IV)
IAE (PSO)	0.9168	1.2635	1.1803	1.0656
IAE (GWO)	0.9118	1.26	1.1790	1.0639

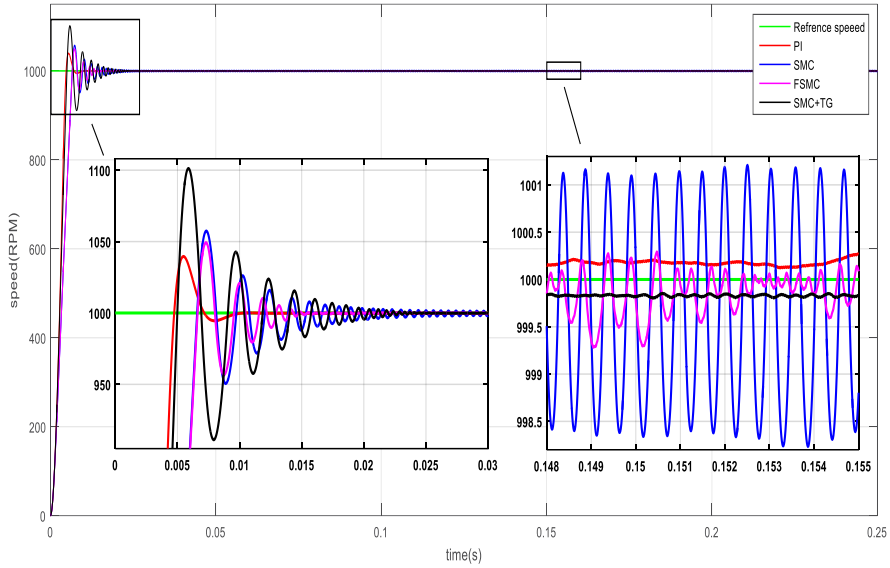

Fig. 7. Reference and actual speed for all scenarios

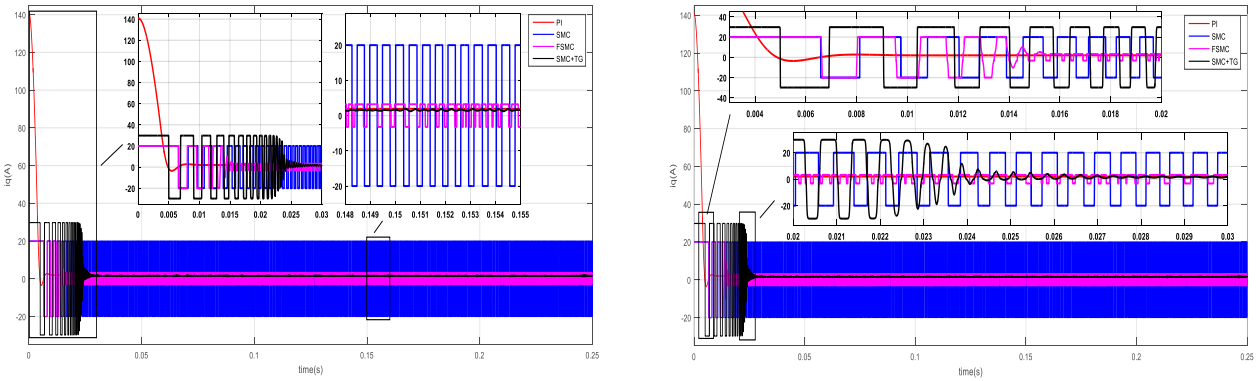

Fig. 8. Reference q-axis current (control signal) for all scenarios

performance than SMC and its advanced counterparts. To select the superior controller between SMC, FSMC and SMC+TG, we review the values recorded for these three controllers in Table 8 and the results in Figs. 7-9. The main drawback of the SMC is the occurrence of the chattering phenomenon that is shown clearly in Figs. 7-9. To reduce this harmful phenomenon, FSMC is used instead of SMC in the speed control loop. Regarding the values recorded in Table 8, when SMC is replaced by FSMC, it causes to increase in T_r and $|e_{ss}|$, but FSMC has managed to reduce T_s and $\%O_s$, and especially the amount of control effort. Meanwhile, Figs. 7-9 demonstrate that chattering has diminished dramatically. Thus, FSMC is a good alternative to SMC in the speed control loop.

In order to further reduce chattering, FSMC is replaced by SMC+TG in the speed control loop. Table 8 shows that this replacement results in increasing of T_s and $\%O_s$, and in contrast, results in decreasing T_r, $|e_{ss}|$ and *IAC*. However, the most important advantage of SMC+TG is the complete elimination of chattering. In order to have a better comparison between scenarios II-IV, based on Fig. 8 which has been appropriately magnified, it can be deduced that for the SMC+TG chattering starts at 4.98msec and completely restrains at 28msec. For the FSMC, chattering starts at 6.603msec and at 15.449msec

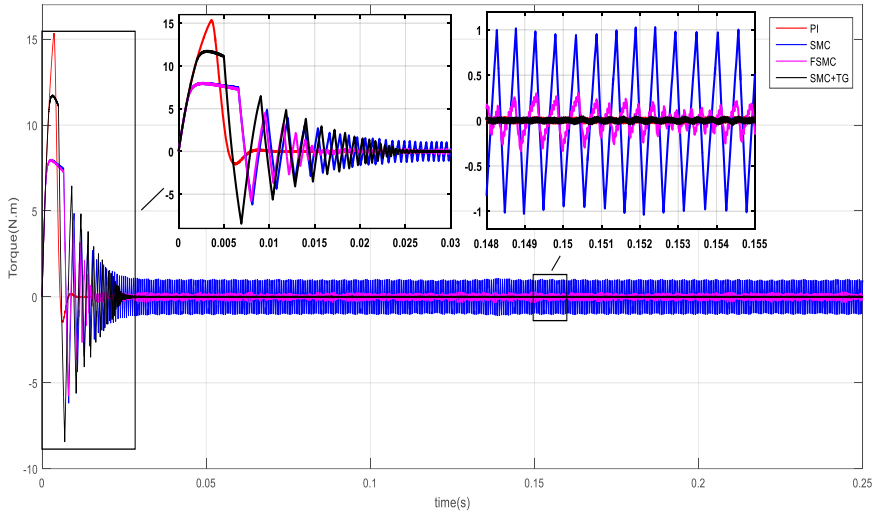

Fig. 9. Electromagnetic torque for all scenarios

Table 8. Characteristics of the speed response and IAC criterion for all scenarios

	T_r (msec)	T_s (msec)	$\%O_s$	$\lvert e_{ss}\rvert$	IAC
PI controller (Scenario I)	4.74	6.336	3.9574	0.1076	0.8797
SMC (Scenario II)	6.587	11.735	5.7399	0.062	5.0001
FSMC (Scenario III)	6.624	11.093	4.9281	0.0671	1.0319
SMC+TG (Scenario IV)	4.992	13.702	10.1202	0.0555	1.0251

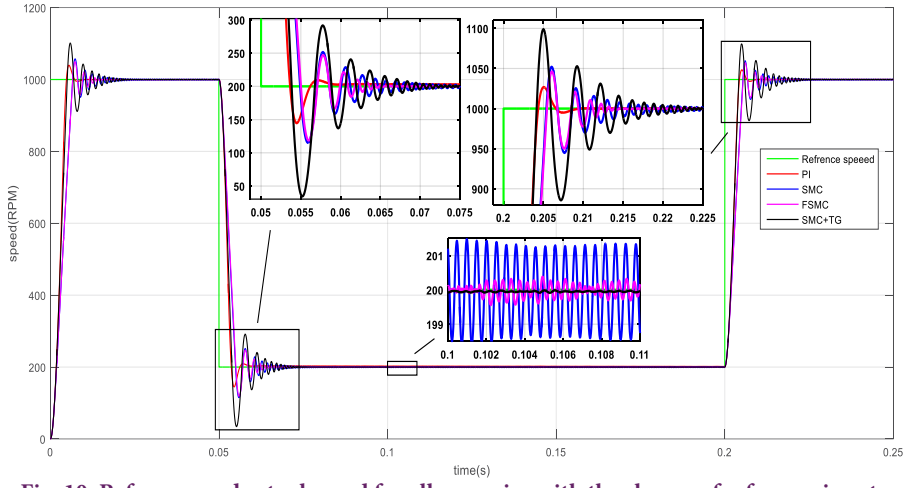

Fig. 10. Reference and actual speed for all scenarios with the change of reference input

declines significantly but is not fully restrained and for the SMC, chattering starts at 6.586msec and it never stops. The electromagnetic torque plots for all four scenarios are depicted in Fig. 9. In this Figure, the chattering effect is observed as permanent fluctuations for SMC and FSMC. Consequently, by ignoring the slight increase in T_s and $\%O_s$, SMC+TG is selected as a suitable alternative for FSMC.

Remark 3. As a conclusion of this subsection, scenarios II-IV do not have significant superiority than scenario I. Scenarios II-IV are able to reach to a better $|e_{ss}|$, while scenario I has fastest response while using minimum control effort.

4.3. Robustness analysis

In subsection 4.2, no uncertainty has been considered, however the PMSM drive suffers from different kinds of uncertainties. To have a thorough comparative analysis the

Table 9. Characteristics of the speed response for all scenarios in tracking 200rpm (changing desired speed from 1000rpm to 200rpm)

	T_r (msec)	T_s (msec)	$\%U_s$	$\lvert e_{ss}\rvert$
PI controller (Scenario I)	3.648	8.681	27.6584	0.4661
SMC (Scenario II)	4.906	19.549	42.4860	0.4303
FSMC (Scenario III)	5.013	13.905	40.7541	0.0419
SMC+TG (Scenario IV)	3.844	20.04	82.8017	0.0147

Table 10. Characteristics of the speed response for all scenarios in tracking 1000rpm (changing desired speed from 200rpm to 1000rpm)

	T_r (msec)	T_s (msec)	$\%O_s$	$\lvert e_{ss}\rvert$
PI controller (Scenario I)	4.348	5.567	2.6812	0.0486
SMC (Scenario II)	5.37	10.62	5.2091	0.5086
FSMC (Scenario III)	5.451	10.123	4.6146	0.1768
SMC+TG (Scenario IV)	4.151	13.748	9.8942	0.0545

robustness of the controllers should also be studied under different uncertainties. The uncertainties studied in this paper include; changing the reference speed, adding external load torque and changing in system inertia that are defined in subsection 4.3.1, 4.3.2 and 4.3.3, respectively.

4.3.1. Changes in reference speed

To evaluate the ability of each scenario to track different reference speeds two different conditions are considered.

A. Condition One

The speed at 0.05sec is decreased from 1000rpm to 200rpm and is increased from 200rpm to 1000rpm at 0.2sec. In Fig. 10, the speed response is plotted for each of the four scenarios, revealing that each of the four scenarios has succeeded in coping with changes in the desired speed. The characteristics of the speed response at 0.05sec and 0.2sec are shown in Tables 9 and 10, respectively. It should be noted that $\%U_s$ in Table 9 denotes the percentage of maximum undershoot and 2% criterion is used to calculate T_s in Tables 9 and 10. Meanwhile, $|e_{ss}|$ in Table 9 is the absolute steady state error between the actual speed and 200rpm while in Table 10 it denotes the absolute steady state error between actual speed and 1000rpm.

At the beginning, the performance of the PMSM drive under three sliding mode controllers (scenarios II-IV) is studied. By comparing the results recorded in Tables 9 and 10, it can be concluded that when SMC is replaced by FSMC, it causes to increase in T_r, but instead, it decreases T_s, $\%O_s$, $\%U_s$ and $|e_{ss}|$. Besides, Fig. 10 indicates a sharp decrease in oscillations of the speed response. The above discussions are sufficient reasons for advantage of FSMC over SMC.

Based on Tables 9 and 10, by replacement of FSMC with SMC+TG in the speed control loop, T_s, $\%O_s$, $\%U_s$ are increased and T_r and $|e_{ss}|$ are decreased. Meanwhile, the oscillations in speed response are totally restrained according to Fig. 10. Considering the importance of the ability of the controller to remove oscillations in motor speed, as well as tracking the desired speed more accurately it can be concluded that SMC+TG is an appropriate alternative to FSMC.

In the case of scenario I, from the results in Table 9 it can be concluded that PI controller than other speed controllers has gained better results in *Tr*, *Ts* and *%Us* and only has not been able to achieve the best result in reducing the amount of $|e_{ss}|$. Besides, recorded results in Table 10 shows that PI controller (scenario I) decreases *Ts*, *%Os* and *|ess|* in comparison to scenarios II-IV and only in comparison to scenario IV increases *Tr*.

B. Condition Two

The speed at 0.05sec is increased from 1000rpm to 1800rpm and is decreased from 1800rpm to 1000rpm at 0.2sec. Fig. 11, shows the speed response of the motor for all scenarios. Like the condition one, each of the four speed controllers has succeeded in tracking the reference speed despite changing in operating point. The characteristics of the speed curve at 0.05sec and 0.2sec are shown in Tables 11 and 12, respectively. As can be seen from Fig. 11 the speed

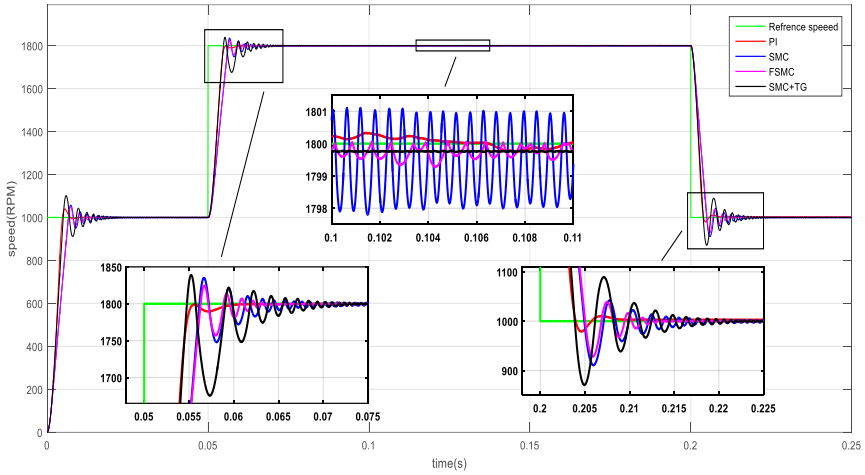

Fig. 11. Reference and actual speed for all scenarios with the change of reference input

Table 11. Characteristics of the speed response for all scenarios in tracking 1800rpm (changing desired speed from 1000rpm to 1800rpm)

	Tr (msec)	*Ts* (msec)	%*Os*	|*ess*|
PI controller (Scenario I)	3.163	4.625	-	0.1133
SMC (Scenario II)	6.172	8.576	1.9455	0.2903
FSMC (Scenario III)	6.309	8.314	1.3621	0.1009
SMC+TG (Scenario IV)	4.772	11.391	2.1591	0.0745

Table 12. Characteristics of the speed response for all scenarios in tracking 1000rpm (changing desired speed from 1800rpm to 1000rpm)

	Tr (msec)	*Ts* (msec)	%*Us*	|*ess*|
PI controller (Scenario I)	3.966	4.749	2.0915	0.7737
SMC (Scenario II)	4.93	11.772	8.9181	0.4874
FSMC (Scenario III)	5.024	9.173	7.1801	0.0841
SMC+TG (Scenario IV)	3.862	14.058	12.9179	0.0505

response using PI controller at 0.05sec is over-damped and thus the time required for the response to rise from 10% to 90% of its final value is considered as *Tr*. It should be noted in Tables 11 and 12, 2% criterion is used to calculate *Ts*. Furthermore, $|e_{ss}|$ in Table 11 is the absolute steady state error between the actual speed and 1800rpm while in Table 12 it denotes the absolute steady state error between actual speed and 1000rpm.

At the beginning, the performance of the PMSM drive using three sliding mode controllers (scenarios II-IV) is compared.

Tables 11 and 12 show that when SMC is replaced by FSMC in the speed control loop, it causes to increase in *Tr*, but it decreases *Ts*, %*Os*, %*Us* and |*ess*|, also from Fig. 11 it is clear that the undesired fluctuations of speed response is decreased. According to this discussion, FSMC is preferable to SMC.

The results recorded in Tables 11 and 12 indicate that replacing FSMC by SMC+TG in the speed control loop increases *Ts*, %*Os* and %*Us*, but decreases *Tr* and |*ess*|. Furthermore, the oscillations in speed response in Fig. 11 have completely diminished that is desirable. Therefore, it is better to replace FSMC with SMC+TG.

At the end, we look at the PI controller (scenario I). The recorded results in Table 11 for *Tr*, *Ts* and %*Os* shows the scenario I has gained the most favorable values than the others. However, scenario I is not able to reduce error as much as the scenarios III and IV. Besides, Tables 12 shows scenario I compared to scenarios II-IV decreases *Ts*, and

%*Us* but increases |*ess*|. Meanwhile, in the case of *Tr*, the results recorded in Table 12 show that scenario I compared to scenarios II and III decreases *Tr*, and compared to scenario IV increases *Tr*.

Remark 4. From conditions one and two it can be seen that no scenario has the best robust performance considering all criteria, but roughly speaking it can be stated that scenario I has the best robust performance against changing reference speed. It should be noted that among scenarios II-IV, scenario IV has the best robust performance, while scenario II has the worst.

4.3.2. Adding external load torque

One of the most important uncertainties for the PMSM drive is the presence of the external load torque. Here, we assume a 4N.m external load torque according to Fig. 12, which is applied to the motor at 0.07sec and is taken off at 0.2sec. It should be noted that the proposed scenarios do not know the value of external load torque in advance and the value here is just for simulation. Fig. 13 is the speed response for all the four scenarios. In order to have better comparison Fig. 13 is magnified and depicted in Fig. 14. Besides, the reference q-axis current and electromagnetic torque are depicted in Figs. 15 and 16, respectively. It can be seen that the robust performance of PI controller (scenario I) is too poor to be studied. Therefore, the performance of the last three scenarios will be studied. The characteristics of speed transient response at 0.07sec and IAC criterion for the last three scenarios are listed in Table 13. It should be noted that to achieve better results to calculate T_s in Table 13, 1% criterion is considered.

Based on Fig. 14 and the values recorded in Table 13 for scenarios III and IV, it can be deduced that SMC+TG in comparison to FSMC reduces $\%U_s$, T_r and $|e_{ss}|$, but, increases IAC and T_s. From Fig. 14 although FSMC has slightly less oscillation than SMC+TG it failed to reach the desired speed. However, SMC+TG has been able to meet the desired speed. Considering the above reasons SMC+TG is more preferable than FSMC. The comparison between scenarios II and IV shows that when SMC is replaced with SMC+TG, it increases $|e_{ss}|$ and T_s, but it decreases T_r, $\%U_s$ and IAC. Last but not least, the use of SMC+TG instead of SMC eliminates the chattering and thus eliminates the oscillations and permanent pulses in the motor output curves. This is well illustrated in Figs. 14-16. For these reasons, SMC + TG is also more preferable than SMC.

Remark 5. To conclude this Subsection, we can state that scenario I is not able to cope with sudden load torque and thus has a poor robust performance. On the other hand, scenario IV has more preferable robust performance in the presence of sudden load torque than scenarios II and III.

4.3.3 Changes in motor's inertia

In order to study the robustness of the proposed speed controllers against parametric uncertainty, the value of the motor's inertia has been tripled. The speed response, reference q-axis current and electromagnetic torque for all scenarios

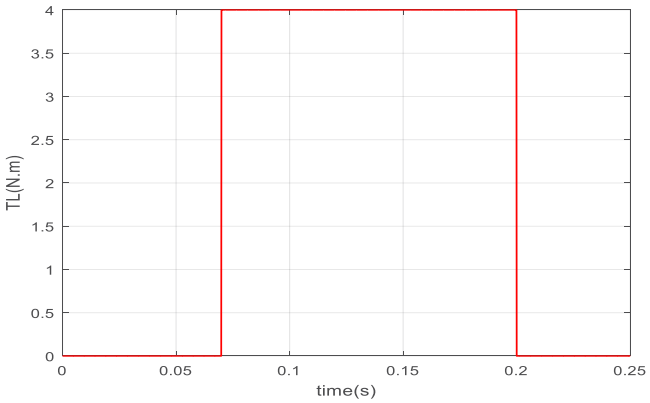

Fig. 12. External load torque

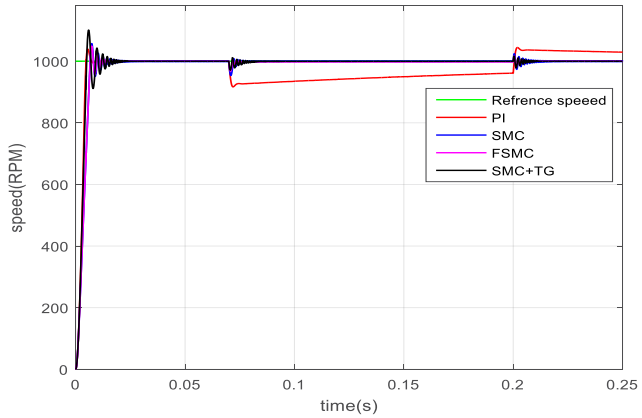

Fig. 13. Reference and actual speed for all scenarios in the presence of load torque.

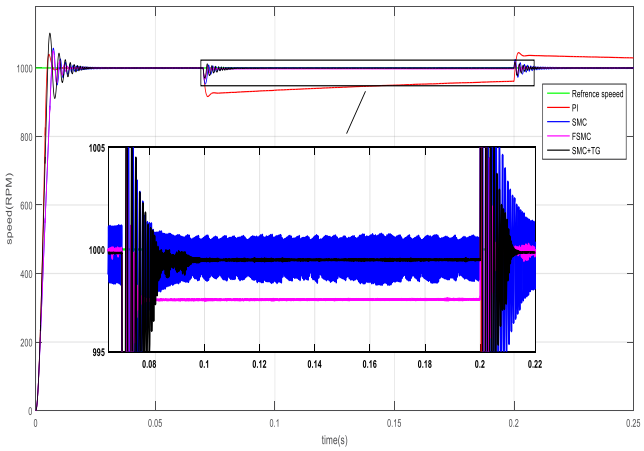

Fig. 14. Magnification of Fig. 13 for better comparison

are depicted in Figs. 17-19, respectively. Furthermore, the characteristics of the speed response and IAC criterion are specified in Table 14. It should be noted that to achieve better results to calculate T_s in Table 14, 1% criterion is considered.

First, the robust performance of SMC, FSMC and SMC+TG is compared and the superior controller is selected. In accordance with the values recorded in Table 14, using

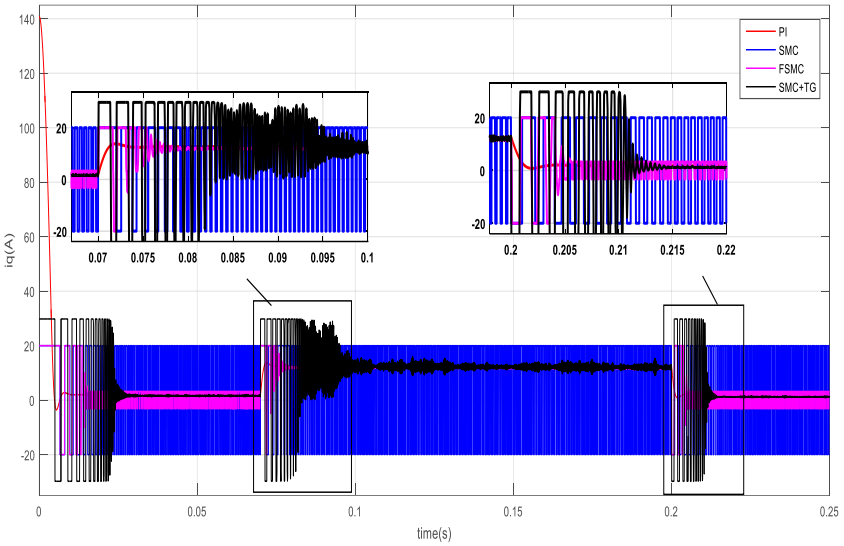

Fig. 15. Reference q-axis current for all scenarios in the presence of load torque

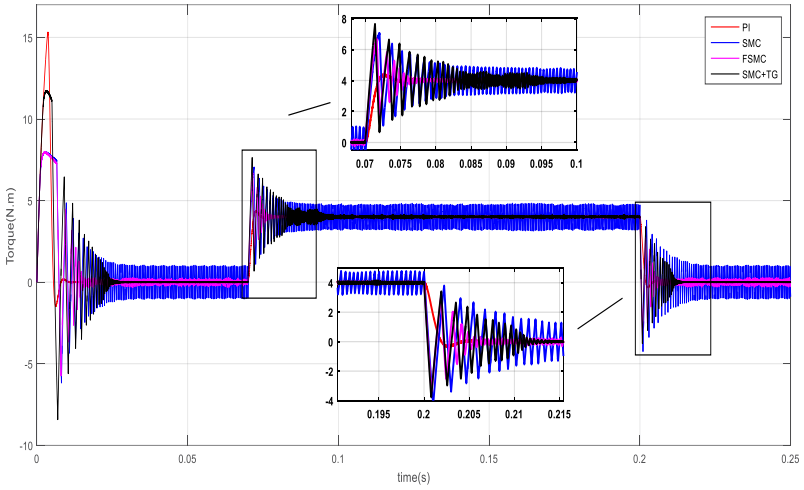

Fig. 16. Electromagnetic torque for all scenarios in the presence of load torque

Table 13. Characteristics of the speed response and IAC criterion for the last three scenarios in the presence of load torque

	T_r (msec)	T_s (msec)	$\%U_s$	IAC	$\lvert e_{ss}\rvert$
SMC (Scenario II)	2.032	4.863	4.6609	5.0002	0.0379
FSMC (Scenario III)	1.673	2.853	3.2238	2.2306	0.1072
SMC+TG (Scenario IV)	1.394	5.955	2.9484	2.9134	0.0495

FSMC instead of SMC in the speed control loop, increases T_r, while decreases T_s, $\%O_s$ and $|e_{ss}|$. Besides, FSMC is able to significantly reduce IAC. On the other hand, from Figs. 17 and 18 it can be seen that the chattering by using FSMC in the speed control loop has been significantly decreased in comparison of using SMC. Thus, FSMC can be considered as a good alternative to SMC in the speed control loop. Based on Table 14, using SMC+TG instead of FSMC increases $\%O_s$ and $|e_{ss}|$ but in contrast decreases T_r, T_s and IAC. In addition, according to Figs. 17 and 18, FSMC significantly has reduced chattering in comparison to SMC but could not completely eliminate it, while SMC+TG has fully removed chattering. Besides, from Fig. 19 it can be seen that the electromagnetic torque oscillations by using FSMC instead of SMC have been

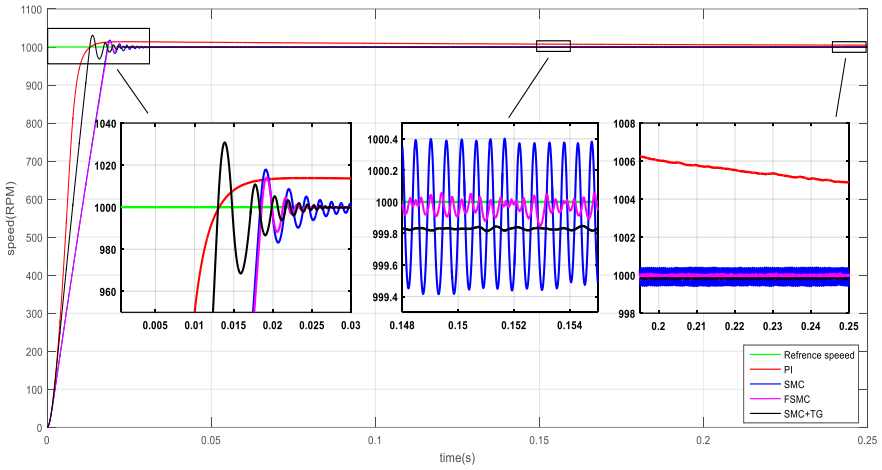

Fig. 17. Reference and actual speed for all scenarios in the presence of inertia change

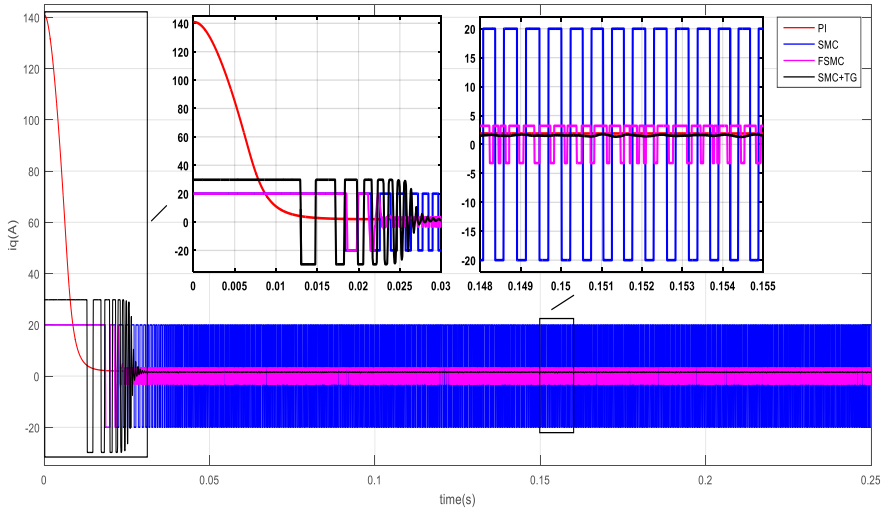

Fig. 18. Reference q-axis current for all scenarios in the presence of inertia change

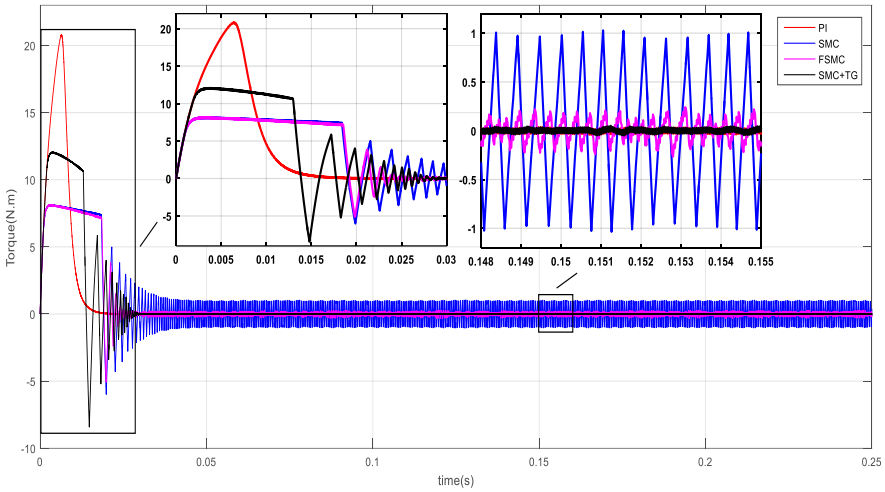

Fig. 19. Electromagnetic torque for all scenarios in the presence of inertia change

greatly decreased, while they will be completely removed if SMC+TG is utilized. According to the above discussions, SMC+TG is more preferable than FSMC, and thus, scenario IV wins the race from scenarios II and III.

Table 14. Characteristics of the speed response and IAC criterion for all scenarios in the presence of inertia change

	T_r (msec)	T_s (msec)	$\%O_s$	$\lvert e_{ss}\rvert$	IAC
PI controller (Scenario I)	13.141	95.995	1.3842	1.533	1.2804
SMC (Scenario II)	18.397	21.215	1.7844	0.1493	5.0001
FSMC (Scenario III)	18.589	20.821	1.4059	0.0233	1.1728
SMC+TG (Scenario IV)	12.995	19.422	3.0763	0.0533	1.0962

Now, we compare scenarios I and IV. From Table 14, it can be seen that using SMC+TG instead of PI controller increases $\%O_s$, but causes significant reduction in $|e_{ss}|$ and T_s. Meanwhile, a decrease happens in T_r and IAC. In addition, Fig. 17 shows that when the PI controller is included in the speed control loop, tracking of the desired speed is poor and very slow which is not acceptable in accurate applications. Therefore, PI controller cannot provide the main purpose of the system, which is following the desired speed with the lowest error possible. Thus, we can conclude that scenario IV has the best robust performance between all scenarios in the presence of inertia change.

Remark 6. As a conclusion in inertia change, it can be seen that the scenario I does not have satisfactory robust performance in accurate applications. It is noteworthy that scenario III has better robust performance and mitigating chattering than scenario II. However, scenario IV has the best robust performance while removing chattering effectively.

Remark 7. Based on Theorems 1 and 2 in Subsections 2.2 and 2.3 the closed-loop nominal stability is guaranteed for SMC , FSMC and SMC+TG if the constants k_c, k_t and δ are considered positive and $0 < \varepsilon < 1$. These constraints are all satisfied by considering the search intervals proposed in Subsection 4.1. Besides, in order to guarantee robust stability, the upper bounds for these parameters are chosen to give the controllers enough robustness. It should be noted that if the uncertainties become larger the upper bounds should be increased. Therefore, the PSO and GWO algorithms search the optimal values of the parameters in the region of stability, which can guarantee both nominal and robust stability. However, for PI controller since we have a highly nonlinear system, finding the region of stability is a difficult task. In this paper, the search interval for PI controllers is obtained by some trial and error procedure.

5. Conclusion

In this paper, operation of the permanent magnet synchronous motor (PMSM) drive has been studied by applying four different speed controllers in field oriented control (FOC) method. These four controllers are: proportional-integral (PI) controller, sliding mode controller (SMC), fuzzy sliding mode controller (FSMC) and sliding mode controller with time-varying switching gain (SMC+TG). In this paper, in order to fairly compare the performance and robustness of these controllers, an optimization framework is proposed. The proposed framework defines an optimization problem to derive the sub-optimal values for the parameters of the controllers. Since the objective is tracking a pre-defined reference speed, to drive parameters of all four speed controllers, integral absolute speed tracking error (IAE) has been considered as a cost function. The defined optimization problem is highly nonlinear and cannot be easily solved, so particle swarm optimization (PSO) and gray wolf optimization (GWO) algorithms have been utilized. For a complete comparison of performance and robustness of the four scenarios, different situations have been considered such as large changes in reference speed, adding external load torque and change in system inertia. Simulation results indicate that a single controller cannot provide a superior speed response for all conditions. Indeed, despite all the efforts have been done to replace PI controller with SMC and its advanced counterparts, it cannot be stated that the sliding mode controllers behave better than the PI controller in all conditions.

References

[1] L. Wang, S. Chai, D. Yoo, L. Gan, K. Ng, PID and Predictive Control of Electrical Drives and Power Converters Using MATLAB / Simulink, Wiley, 2015.

[2] S. Sivanagaraju, M.B. Reddy, A.M. Prasad, Power Semiconductor Drives, Prentice-Hall Of India Pvt. Limited, 2009.

[3] H. Abu-Rub, A. Iqbal, J. Guzinski, ebrary Inc., High performance control of AC drives with MATLAB/Simulink models, Wiley, Chichester, West Sussex ; Hoboken, NJ, 2012.

[4] G.R. Slemon, Electrical machines for variable-frequency drives, Proceedings of the IEEE, 82(8) (1994) 1123-1139.

[5] X.d.T. Garcia, B. Zigmund, A.A. Terlizzi, R. Pavlanin, L. Salvatore, Comparison between FOC and DTC strategies for permanent magnet synchronous motors, Advances in Electrical and Electronic Engineering, 5(1) (2011) 76-81.

[6] Z. Ibrahim, E. Levi, A comparative analysis of fuzzy logic and PI speed control in high-performance AC drives using experimental approach, IEEE Transactions on Industry Applications, 38(5) (2002) 1210-1218.

[7] Q. Song, C. Jia, Robust speed controller design for permanent magnet synchronous motor drives based on sliding mode control, Energy Procedia, 88 (2016) 867-873.

[8] F. Piltan, N.B. Sulaiman, Review of sliding mode control of robotic manipulator, World Applied Sciences Journal, 18(12) (2012) 1855-1869.

[9] W. Gao, J.C. Hung, Variable structure control of nonlinear systems: A new approach, IEEE transactions on Industrial Electronics, 40(1) (1993)

45-55.
[10] C.-C. Fuh, Variable-thickness boundary layers for sliding mode control, Journal of Marine Science and Technology, 16(4) (2008) 288-294.
[11] J.J.E. Slotine, W. Li, Applied nonlinear control, Prentice-Hall, Englewood Cliffs,N.J., 1991.
[12] J. Burton, A.S. Zinober, Continuous approximation of variable structure control, International journal of systems science, 17(6) (1986) 875-885.
[13] M.-S. Chen, Y.-R. Hwang, M. Tomizuka, A state-dependent boundary layer design for sliding mode control, IEEE transactions on automatic control, 47(10) (2002) 1677-1681.
[14] T.-L. Chern, Y.-C. Wu, Design of integral variable structure controller and application to electrohydraulic velocity servosystems, in: IEE Proceedings D (Control Theory and Applications), IET, 1991, pp. 439-444.
[15] H. Alli, O. Yakut, Fuzzy sliding-mode control of structures, Engineering Structures, 27(2) (2005) 277-284.
[16] H. Lee, E. Kim, H.-J. Kang, M. Park, A new sliding-mode control with fuzzy boundary layer, Fuzzy Sets and Systems, 120(1) (2001) 135-143.
[17] M.R. Becan, Sliding Mode Control with Fuzzy Boundary Layer to Air-Air Interception Problem, in: IEC (Prague), 2005, pp. 108-111.
[18] G. Bartolini, A. Ferrara, A. Levant, E. Usai, On second order sliding mode controllers, in: Variable structure systems, sliding mode and nonlinear control, Springer, 1999, pp. 329-350.
[19] A. Attou, A. Massoum, E. Chiali, Sliding mode control of a permanent magnets synchronous machine, in: 4th International Conference on Power Engineering, Energy and Electrical Drives, IEEE, 2013, pp. 115-119.
[20] Y. Liu, B. Zhou, H. Wang, S. Fang, A new sliding mode control for permanent magnet synchronous motor drive system based on reaching law control, in: Industrial Electronics and Applications, 2009. ICIEA 2009. 4th IEEE Conference on, IEEE, 2009, pp. 1046-1050.
[21] A. Wang, X. Jia, S. Dong, A new exponential reaching law of sliding mode control to improve performance of permanent magnet synchronous motor, IEEE transactions on magnetics, 49(5) (2013) 2409-2412.
[22] X. Zhang, L. Sun, K. Zhao, L. Sun, Nonlinear speed control for PMSM system using sliding-mode control and disturbance compensation techniques, IEEE Transactions on Power Electronics, 28(3) (2013) 1358-1365.
[23] K.A. Prasad, U. Nair, A. Unnikrishnan, Fuzzy sliding mode control of a Permanent Magnet Synchronous Motor with two different fuzzy membership functions, in: Power, Instrumentation, Control and Computing (PICC), 2015 International Conference on, IEEE, 2015, pp. 1-6.
[24] S. Hussain, M.A. Bazaz, Fuzzy integrated sliding mode controller for vector controlled PMSM, in: Power India International Conference (PIICON), 2014 6th IEEE, IEEE, 2014, pp. 1-6.
[25] J. Liu, H. Li, Y. Deng, Torque ripple minimization of PMSM based on robust ILC via adaptive sliding mode control, IEEE Transactions on Power Electronics, 33(4) (2018) 3655-3671.
[26] Y. Jiang, W. Xu, C. Mu, Y. Liu, Improved Deadbeat Predictive Current Control Combined Sliding Mode Strategy for PMSM Drive System, IEEE Transactions on Vehicular Technology, 67(1) (2018) 251-263.
[27] S. Singh, A. Gautam, J. Dubey, J. Pandey, R. Payasi, Performance comparison of PMSM drive using PI and Fuzzy Logic based controllers, in: Electrical, Computer and Electronics Engineering (UPCON), 2016 IEEE Uttar Pradesh Section International Conference on, IEEE, 2016, pp. 563-569.
[28] S. Hussain, M.A. Bazaz, Comparative analysis of speed control strategies for vector controlled PMSM drive, in: Computing, Communication and Automation (ICCCA), 2016 International Conference on, IEEE, 2016, pp. 1314-1319.
[29] S. Li, Z. Liu, Adaptive speed control for permanent-magnet synchronous motor system with variations of load inertia, IEEE Transactions on Industrial Electronics, 56(8) (2009) 3050-3059.
[30] V. Utkin, Variable structure systems with sliding modes, IEEE Transactions on Automatic control, 22(2) (1977) 212-222.
[31] J. Huang, L. Cui, X. Shi, H. Li, Z. Xiang, Composite integral sliding mode control for PMSM, in: Proc. of 33rd Chinese Control Conf., Nanjing, China, 2014, pp. 28-30.
[32] L.-X. Wang, A course in fuzzy systems and control, Prentice Hall, Upper Saddle River, N.J., 1997.
[33] M.B. Ghalia, A.T. Alouani, Sliding mode control synthesis using fuzzy logic, in: American Control Conference, Proceedings of the 1995, IEEE, 1995, pp. 1528-1532.
[34] R. Eberhart, J. Kennedy, A new optimizer using particle swarm theory, in: Micro Machine and Human Science, 1995. MHS'95., Proceedings of the Sixth International Symposium on, IEEE, 1995, pp. 39-43.
[35] D.P. Rini, S.M. Shamsuddin, S.S. Yuhaniz, Particle swarm optimization: technique, system and challenges, International journal of computer applications, 14(1) (2011) 19-26.
[36] Y. Shi, R. Eberhart, A modified particle swarm optimizer, in: Evolutionary Computation Proceedings, 1998. IEEE World Congress on Computational Intelligence., The 1998 IEEE International Conference on, IEEE, 1998, pp. 69-73.
[37] S. Mirjalili, S.M. Mirjalili, A. Lewis, Grey wolf optimizer, Advances in engineering software, 69 (2014) 46-61.
[38] P. Vasant, Meta-heuristics optimization algorithms in engineering, business, economics, and finance, Information Science Reference, 2013.
[39] R. Poli, J. Kennedy, T. Blackwell, Particle swarm optimization, Swarm intelligence, 1(1) (2007) 33-57.

HOW TO CITE THIS ARTICLE

F. Khorsand, R. Shahnazi, E. Fallah, A Thorough Comparative Analysis of PI and Sliding Mode Controllers in Permanent Magnet Synchronous Motor Drive Based on Optimization Algorithms, AUT J. Elec. Eng., 51(2) (2019) 171-186.

DOI: 10.22060/eej.2019.16219.5278